Novel fluorescent nanoprobe based on hyaluronic acid and polyethyleneimine functionalized graphene oxide for detecting hyaluronidase as tumor marker

Ping Zhang, Chaoqun Zhang, Jie Song, Shuxin Wang, Qian Li, Feng Su, Suming Li

Novel fluorescent nanoprobe based on hyaluronic acid and polyethyleneimine functionalized graphene oxide for detecting hyaluronidase as tumor marker

Ping Zhang,[1] Chaoqun Zhang,[1] Jie Song,[1] Shuxin Wang,[1] Qian Li,[21] Feng Su,[1,3]* Suming Li[4]**

[1] College of Chemical Engineering, Qingdao University of Science and Technology, Qingdao 266042, China

[2] Cancer Institute, Affiliated Hospital of Qingdao University, Qingdao, 266071, China

[3] Institute of High Performance Polymers, Qingdao University of Science and Technology, Qingdao 266042, China

[4] Institut Europeen des Membranes, IEM UMR 5635, Univ Montpellier, CNRS, ENSCM, Montpellier, France

***Correspondance**

sufeng@qust.edu.cn (F. Su); liqian123@qdu.edu.cn (Q. Li) ; suming.li@umontpellier.fr (S. Li)

Funding Sources

This research was funded by the Shandong Provincial Natural Science Foundation (ZR2020MH324, ZR2021ME208, ZR2022ME083).

Keywords: Nanoprobe; Hyaluronic acid; Polyethyleneimine; Graphene oxide; Tumor marker.

Abstract

A novel nanoprobe was developed for the detection of hyaluronidase as cancer marker, using fluorescein 5-isothiocyanate (FITC) as fluorescence indicator, hyaluronic acid (HA) and polyethyleneimine (PEI) functionalized graphene oxide (GO) as quencher. PEI was attached to GO through amide bonding, using 1-ethyl-3-(3-dimethylaminopropyl) carbodiimide (EDC) and N-hydroxysuccinimide (NHS) as coupling agents. Aminated hyaluronic acid (HA) was then linked to GO-PEI (GOP) via the same route. NMR, UV-Vis-NIR, FT-IR, SEM and TGA analyses confirmed the successful synthesis of GOP-HA. Finally, FITC was attached to GOP-HA through reaction between the isothiocyanate group of FITC and the amine group of aminated HA. The fluorescence of FITC is quenched in the resulted GOP-HA-FITC nanoprobe. Addition of hyaluronidase can cleave HA chains into small fragments, releasing FITC to emit fluorescence. Importantly, the nanoprobe is highly sensitive and selective, and can enter cells by specifically binding to the CD44 receptor on the surface of Hela cells. Therefore, GOP-HA-FITC nanoprobe could be used in targeted tumor cell imaging for the early diagnosis of cancers.

1. Introduction

Cancer is one of the leading causes of human death in the world. Nearly 10 million people died of cancers in 2020 according to the World Health Organization (WHO). The early diagnosis of cancer is thus of particular importance.[1] The occurrence of cancer is often accompanied by the rise of a variety of indicators, among which enzyme determination has been used to diagnose cancers for half a century. Studies have shown that the increase of Regan isoenzyme of alkaline phosphatase is closely related to the occurrence of occult renal cell carcinoma. The continuous increase after operation indicates the persistence or recurrence of the disease.[2] Leucine aminopeptidase (LAP) is also an important marker for cancer diagnosis as it is overexpressed in many cancers. Chai et al. developed a water-soluble near infrared (NIR) fluorescent probe (CHMC-M-Leu). The probe exhibited high sensitivity and responsiveness to LAP, showed good cell uptake, and was successfully used to monitor endogenous LAP in living cells.[3]

The occurrence, proliferation and metastasis of cancer are also closely related to extracellular matrix (ECM).[4] Hyaluronic acid (HA) is a linear polysaccharide composed of D-glucuronic acid and N-acetyl-D-glucosamine. HA is largely present in the human body as the main component of the ECM. Hyaluronidases are specific hydrolases which can cleave HA chains into small fragments.[5] Many recent studies have shown hyaluronidases are overexpressed in cancers, such as breast cancer, colon cancer and Laryngeal carcinoma.[6-8] A variety of hyaluronidase detection methods have been developed for cancer diagnosis, including viscosity method, turbidimetry, zymography, colorimetry, spectrophotometry, etc.[9-12] However, these methods present some disadvantages such as complex operation, low sensitivity and low selectivity. Therefore, it is necessary to develop

a fast, highly sensitive and selective method for the detection of hyaluronidase, and nanoprobes are one of the possible solutions.

It is well known that HA can specifically bind to the CD44 receptor on the surface of cancer cells. Different nanoprobes for the detection of hyaluronidase have been reported. For example, silicon nanoparticles (SiNPs) and molybdenum disulfide quantum dots (MoS2 QDs) are assembled with HA-functionalized gold nanoparticles (HA-AuNPs) to form a nanoprobe.[13,14] A novel upconversion luminescent nanoprobe was developed by coupling HA upconversion fluorescent nanoparticles (HA-UCNPs) with poly(m-phenylenediamine) (PMPD) nanospheres through covalent bonds.[15] There are also diagnostic and therapeutic probes made from carbon dots (P-CDs) and HA.[16] The fluorescence in nanoprobes is quenched by Förster resonance energy transfer (FRET). With the addition of hyaluronidase, HA chains are cleaved and SiNPs, MoS2 QDs, UCNPs, or P-CDs are released, thereby restoring fluorescence. However, the preparation process of these nanoprobes is tedious and requires high temperature reaction.

Fluorescent nanoparticles have also been developed for the detection or imaging of other cells. Yildiz et al. prepared doxorubicin-loaded NPs from Alexa Fluor 750-labeled poly(lactic-*co*-glycolic acid)-*b*-poly-L-lysine (PLGA-PLL-AF750) and poly(lactic acid)-*b*-poly(ethylene glycol) (PLA-PEG) block copolymers. In vitro studies showed that NPs are able to deliver doxorubicin over a long period of time and have fluorescent activation after interaction with proteolytic enzymes. Cell studies demonstrated the theranostic properties of the NPs as contrast agents for fluorescence imaging and anticancer drugs.[17] Hernandez et al. developed fluorescein isothiocyanate-conjugated poly-D-lysine (PDL-FITC) coated gold nanoparticles (AuNP) which are sensitive to

reactive oxygen species (ROS), and can be used to identify pro-inflammatory macrophages in different cell populations.[18]

Graphene oxide (GO) has been widely studied for biomedical applications because of its unique properties, including two-dimensional planar structure, large surface area, chemical and mechanical stability, excellent conductivity and biocompatibility. Moreover, abundant oxygen-containing functional groups are present on the surface of GO, which is conducive to modification.[19] GO has been widely used in optoelectronics, biomedicine, drug release, tumor treatment, etc.[20,21] A novel drug carrier was designed by modifying GO with polyetheramine (PEA) and hyaluronic acid (HA) to load quercetin.[22] The results showed that the anti-tumor efficacy was enhanced and the effect was longer lasting compared to the use of quercetin alone, suggesting that GO-based materials present good potential for clinical applications.

Polyethyleneimine (PEI) is a cationic polymer containing readily protonated primary, secondary and tertiary amines.[23] It can interact with negatively charged DNA or drugs through electrostatic interaction to form nanocomplexes, and has been widely investigated for uses as a gene or drug carrier. Different from poly(L-lysine) (PLL), PEI is only partially amino protonated at physiological pH, allowing the polymer to act as an effective "proton sponge". However, the cytotoxicity of PEI considerably limits its applications. It has been shown that PEI with a molecular weight (MW) below 2000 Da displays a low cytotoxicity.[24] PEI can also form a compact nanostructure with negatively charged HA through electrostatic adsorption. Rodrigues et al. developed a tumor-targeted chemo-photothermal nanomedicine through functionalization of acridine orange (AO)-loaded gold-core mesoporous silica shell (AuMSS) nanorods with PEI and HA. Functionalization

of the AuMSS nanorods was achieved through the chemical linkage of PEI followed by electrostatic adsorption of HA.[25]

Fluorescein isothiocyanate (FITC) is a derivative of fluorescein widely used to label proteins by reaction of isothiocyanate with amino groups. Hsu et al. synthesized FITC-labeled, HA-coated nanogold (NP-FITC) to carry plasmid or siRNA into mesenchymal stem cells.[26] Cheng et al. prepared FITC-labeled HA (FITC-HA) functionalized fluorescent gold nanoparticles (AuNPs) based nanoprobes (FITC-HA-AuNPs) via chemical reduction of $HAuCl_4$ by using FITC-HA as both a reducing and stabilizing agent.[27] The FITC-HA-AuNPs nanoprobes showed high detection sensitivity and allowed for rapid hyaluronidase detection in complex biological specimens. Nevertheless, AuNPs are unstable in high salinity environment.[28]

The aim of this work was to develop a new FITC labeled nanoprobe. PEI was attached to GO through amide bonding, using 1-ethyl-3-(3-dimethylaminopropyl) carbodiimide (EDC) and N-hydroxysuccinimide (NHS) as coupling agents. Aminated HA was then linked to GO-PEI (GOP) via the same route. Finally, FITC was attached to GOP-HA via reaction between the isothiocyanate group of FITC and the amine groups of aminated HA. The successful synthesis of the fluorescent probe was evidenced by UV-Vis-NIR spectroscopy, nuclear magnetic resonance (NMR), Fourier transform infrared spectroscopy (FTIR), X-ray photoelectron spectroscopy (XPS), thermogravimetric analysis (TGA), and transmission electron microscopy (TEM). The sensitivity of the fluorescent probe to hyaluronidase was determined by detecting the fluorescence characteristics in phosphate buffered saline (PBS) and cancer cells. This probe presents three main advantages. First, GOP-HA is obtained by covalent amide bonding. The preparation process is simple and the amide bond is stable. Secondly, the detection of hyaluronidase has high sensitivity and selectivity. Third,

electrostatic interactions between negatively charged GO and HA with positively charged PEI contribute to stabilize a compact structure of GOP-HA. Scheme 1 illustrates the preparation of nanoprobe and detection of hyaluronidase. FRET leads to fluorescence quenching in FITC labeled GOP-HA probe. Once entered the cancer cells, HA chains are cleaved into small fragments by hyaluronidases. FITC is consequently released, thus restoring fluorescence which indicates detection of hyaluronidase.

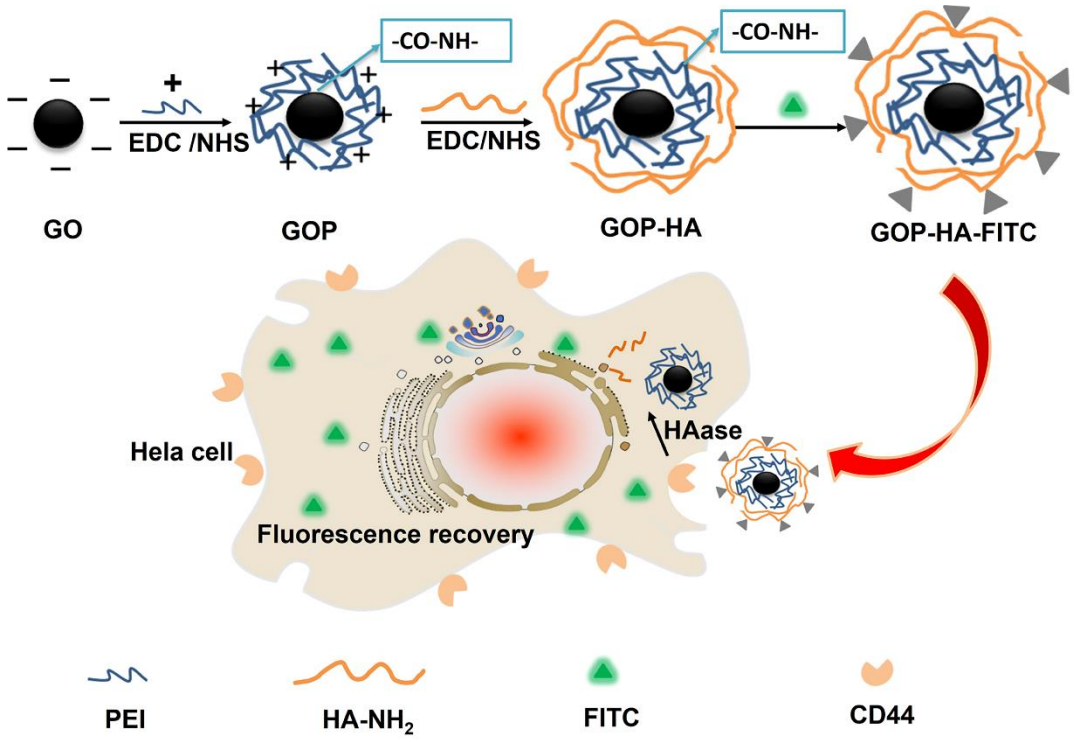

Scheme 1. Synthesis route of GOP-HA-FITC nanoprobe and schematic illustration of hyaluronidase detection.

2. Materials and Methods

2.1 Materials

GO was purchased from Xianfeng NANO Material Tech Co. HA (Mw = 10000) was purchased from Xi'an Lande Biotechnology Co. PEI (Mw = 1800) and cysteine were purchased from McLean reagent network. Ethylenediamine (EDA) monohydrate was purchased from Aladdin Reagent Network. Hyaluronidase (from bovine testis) and protease K were purchased from Beijing Solarbio Science & Technology Co. EDC and NHS were supplied by Shanghai Aladdin Biochemical Technology Co. Bovine serum albumin (BSA) and lysozyme were obtained from Roche Life Science Products. Trypsin was obtained from Thermo Fisher Technology. Collagenase was supplied by Sigma Aldrich. Sodium chloride (NaCl), potassium chloride (KCl), magnesium chloride ($MgCl_2$), calcium chloride ($CaCl_2$), and glucose and vitamin B1 were purchased from Sinopharm Chemical Reagent Co. MTT (3-[4,5-dimethylthiazol-2-yl]-2,5 diphenyl tetrazolium bromide) (98% purity) was purchased from Sigma–Aldrich Co., Ltd. (St. Louis, MO, USA).

2.2 Synthesis of GO-PEI (GOP)

PEI modified GO was prepared by condensation reaction between carboxyl groups of GO and amine groups of PEI, as described in Scheme 2. 20 mg GO was dispersed in 20 mL distilled water, and sonicated for 1 h to obtain a clear suspension. EDC (50 mg) and NHS (75 mg) were added under stirring, and the mixture was stirred for 3 h at room temperature in the dark. 5 mL of 2% PEI solution were then added dropwise under stirring, and the pH of the reaction system was adjusted to 6 with 5% HCl. The reaction proceeded for 48 h at 30 ℃ under stirring, followed by 4 h ultrasonication. Afterwards, the solution was dialyzed against deionized water for 48 h. Finally, PEI modified GO was obtained by centrifugation.

2.3 Synthesis of GO-PEI-HA (GOP-HA)

Aminated HA (HA-NH_2) was synthesized according to a previous report with slight modifications.[29] Briefly, HA (100 mg) was dissolved in 20 mL deionized water. 30 mg EDC and 18 mg NHS were then added. After 30 min activation, 8.4 μL EDA was added, and the mixture was stirred at room temperature for 24 h. Finally the mixture was dialyzed (SpectraPor, MWCO 3.5 kDa) for 48 h, and freeze-dried to yield aminated HA.

HA-NH_2 (10 mg) was dissolved in 10 mL deionized water. EDC (2.5 mg) and NHS (1.5 mg) were then added. After 30 min activation, GOP (20 mg) was added, and the reaction proceeded under stirring at room temperature for 24 h. The reaction mixture was then centrifuged to yield GOP-HA (Scheme 2).

2.4 Characterization

FTIR spectroscopy was performed using a PerkinElmer Spectrum 100 spectrometer in the wavenumber range of 4000-400 cm^{-1}, with a resolution of 1 cm^{-1}. UV-Vis-NIR spectroscopy was carried out with Shimadzu UV-2450 in the detection wavelength range of 200-800 nm. ^{1}H-NMR spectra were registered on an AVANCE 500MHZ NMR spectrometer, using D_2O as solvent. TEM was performed by using JEM-2100 electron microscope. One drop of 1 mg/mL GOP or GOP-HA suspension was placed on a copper grid covered with nitrocellulose membrane, and air dried before measurement. Zeta potential of samples in distilled water was measured by using Malvern Zetasizer Nano ZS. XPS was performed using a Thermo ESCALAB 250 photoelectron spectrometer. Measurements were made with a dual anode aluminum Kα X-ray source (1486 eV, 300 watts). TGA was carried out using NETZSCH STA 449F3 thermogravimetric analyzer. Measurements were made in the temperature range from 50 to 800°C at a heating rate of 5 °C/min under air flow at 100 mL/min. Fluorescence intensity was measured by using an F-4600 FL spectrofluorometer in the

wavelength range of 400-800 nm. Cell imaging was achieved on an Olympus CKX41 fluorescence microscope by the B excitation path, using a 50W mercury lamp, a DM500 beamsplitter, a BP460-490C excitation filter and a BA520 IF absorption filter, respectively.

2.5 Preparation of GOP-HA-FITC

10 mg GOP-HA was dispersed in 2 mL distilled water. 0.1 mg FITC was then added. The reaction proceeded for 24 h under magnetic stirring. The reaction mixture was then dialyzed against distilled water for three days (MWCO = 3500) to remove unconnected fluorescent molecules. After dialysis, the suspension was irradiated with ultraviolet lamp to ensure that there was no residual fluorescence, and finally lyophilized for 48 h in a freeze dryer to yield GOP-HA-FITC in the form of a powder (Scheme 2).

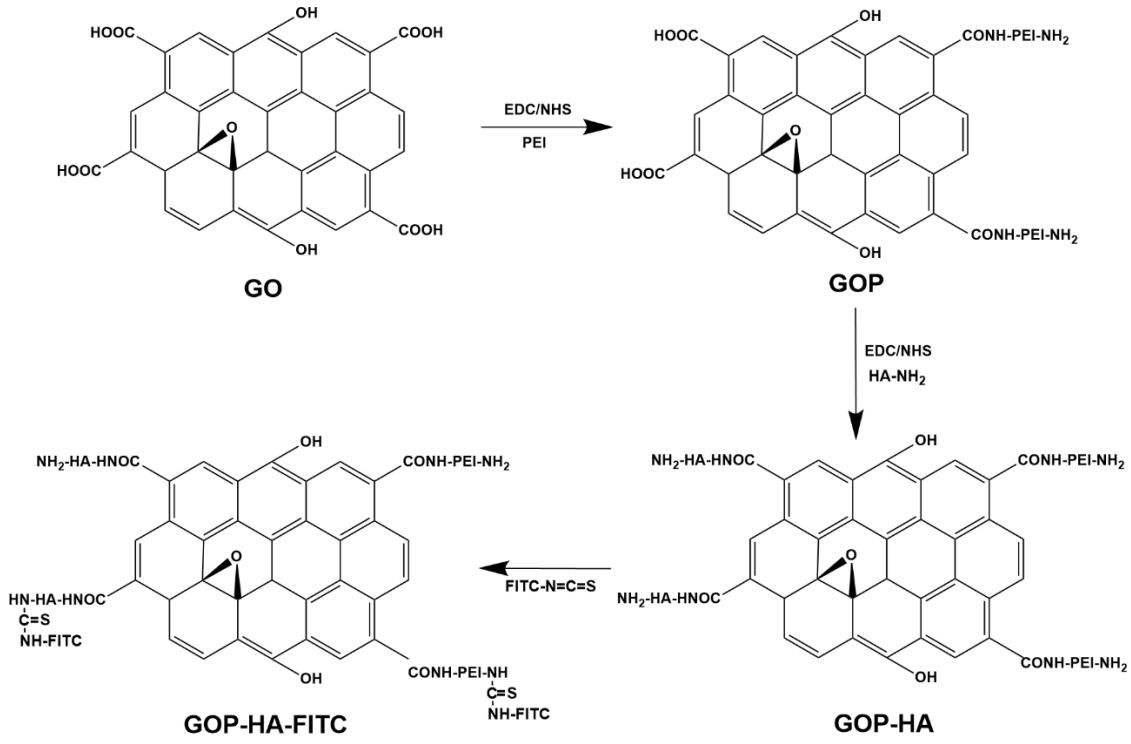

Scheme 2. Synthesis route of GOP-HA-FITC synthesis in 3 steps: 1) synthesis of GO-PEI (GOP) by attachment of PEI to GO via amide bonding, using EDC/NHS as coupling agents, 2) synthesis

of GOP-HA via amide bonding of aminated HA to GOP, 3) synthesis of GOP-HA-FITC via reaction between the isothiocyanate group of FITC and the amine groups of aminated HA.

2.6 Fluorescence quenching test

FITC, GOP-HA-FITC (in duplicate), and mixture of GOP-HA-FITC with hyaluronidase were separately dispersed in 2 mL pH 7.4 PBS. The concentration of FITC, GOP-HA-FITC and hyaluronidase was 0.05 mg/mL, 0.05 mg/mL and 2.5 U/mL, respectively. One of the two GOP-HA-FITC solutions and the mixture solution were incubated at 37 ℃ for 3 h. The fluorescence spectra of the solutions were recorded by using fluorescence spectrophotometer under 490 nm excitation.

2.7 Effect of enzyme concentration

0.1 mg GOP-HA-FITC nanoprobe and various amounts of hyaluronidase were added to 2 mL pH 7.4 PBS. The hyaluronidase concentration was 0, 0.05, 0.1, 0.25, 1, 2.5, 5, 7.5, 10, 12.5 and 15 U/mL, respectively. The solutions were incubated for 3 h at 37℃ in the dark. The fluorescence intensity of the various solutions was then recorded at an excitation wavelength of 490 nm.

2.8 Effect of incubation time

0.1 mg of GOP-HA-FITC nanoprobe was dispersed in 2 mL pH 7.4 PBS. Hyaluronidase is then added at a concentration of 10.0 U/mL. The fluorescence intensity of the solutions was measured after incubation at 37℃ in the dark for 0, 30, 60, 90, 120, 180 min. Three parallel measurements were made for each data point.

2.9 Stability tests of GOP-HA-FITC nanoprobe

A series of NaCl solutions at different concentrations (0, 10, 100, 500, 750, 1000 mM) were prepared. Complete media for cell culture were prepared from DMEM and 1640 medium purchased

from Solebao Reagent Network with 10% fetal bovine serum. 0.1 mg nanoprobe was added into 2 mL of NaCl solutions or cell culture media, and the final probe concentration was 0.05 mg/mL. After 3 h incubation in the dark with hyaluronidase (2.5 U/mL), the fluorescence of the various solutions was measured by using a fluorescence spectrophotometer under 490 nm excitation.

0.1 mg of fluorescent probe was added into 2 mL of PBS solutions of different pH values (3, 4, 5, 6, 7, 8, 9). Hyaluronidase (2.5 U/mL) was then added. After 3 h incubation at 37°C in the dark, the fluorescence of the solutions was determined.

0.1 mg of GOP-HA-FITC nanoprobe was suspended in 2 mL of pH 7.4 PBS. The solutions were exposed to UV light for 30, 60, 90, 120, 150, and 180 min. Hyaluronidase (2.5 U/mL) was then added. The various solutions were incubated in the dark at 37°C for 3 h, and the fluorescence was measured.

All stability measurements were made in triplicate.

2.10 Selectivity evaluation

Different competing species were used to evaluate the selectivity of the nanoprobe, including thrombin, bovine serum albumin, KCl, sodium chloride, lysozyme, cysteine, alkaline phosphatase, glucose, cytochrome c, trypsin and glutathione. 0.1 mg of GOP-HA-FITC nanoprobe was added in 2 mL solution of the competitor species. The concentration of both the nanoproble and competing species was 0.05 mg/mL. The mixture was incubated in a shaker for 3 h in the dark. Then the fluorescence intensity was recorded. Triplicate measurements were made for all competing species.

2.11 MTT, hemolysis and coagulation assays

L929 mouse fibroblasts were diluted to a concentration of $1x10^5$ cells/mL with DMEM (10% calf serum, 100 μg/mL Penicillin, 100 μg/mL streptomycin). 100 μL cell suspension was added to

each well of 96-well plates. The cells were cultured in a CO_2 incubator for 24 h to allow cell adhesion. The nanoprobe was sterilized by exposure to UV light for 30 min and then dispersed in DMEM. The solution was then removed and 100 μL of fresh medium containing GOP-HA-FITC at various concentrations (10, 30, 50, 70, 100 μg/mL) were added to each well. Cells in pure medium and in 0.5% phenol solution were used as negative and positive controls, respectively. After 24 and 72 h incubation, the solution was removed, and 100 μL medium and 20 μL MTT solution (5 mg/mL) were added to each well. The solution was removed after 4 h incubation, and 150 μL dimethyl sulfoxide (DMSO) was added. After 5 min homogenization, the OD value was measured at 490 nm by using microplate reader (Elx800; BioTek, USA). All experiments were performed in triplicate. The cell viability was calculated according to the following formula:

$$\text{Cell viability (\%)} = \frac{\text{OD}_{\text{test}}}{\text{OD}_{\text{negative}}} \times 100\% \qquad \text{(eq. 1)}$$

Whole blood was obtained from four week old new Zealand rabbit by phlebotomy, and collected in an anticoagulant tube containing EDTA. After homogenization, the mixture was centrifuged at 3000 rpm for 15 min to obtain blood cells. 20 μL of blood cells were separately mixed with 1 mL of nanoprobe solution at different concentrations (25, 50, and 100μg/mL). Physiological saline and distilled water were used as negative and positive controls, respectively. The mixtures were incubated at 37°C for 4 h, and then centrifuged at 3000 rpm for 15 min. The supernatant was transferred into a 96-well plate, and the absorbance was measured at 540 nm with a microplate reader. Three parallel measurements were made for each group. The hemolysis rate was calculated according to the following formula:

$$\text{Hemolysis rate (\%)} = \frac{\text{OD}_{\text{test}} - \text{OD}_{\text{negative}}}{\text{OD}_{\text{positive}} - \text{OD}_{\text{negative}}} \times 100\% \qquad \text{(eq. 2)}$$

Whole blood was obtained from four week old new zealand rabbit by phlebotomy. It was collected in an anticoagulant tube containing EDTA. At the same time, 0.2 M $CaCl_2$ solution was prepared and sterilized at high temperature. Lyophilized nanoprobe was added in a $CaCl_2$ solution to prepare suspensions of different concentrations (25, 50, 100μg/mL), and 25 μl of nanoprobe suspension were pipetted into a siliconized glass tube. Siliconized glass tube was selected as the negative control, and unsilanized glass tube as the positive control. After 5 min incubation at 37°C, 0.2 mL of fresh anticoagulant were added to each test sample and homogenized. At predetermined time points, 20 mL of distilled water were added to the test tube, and the OD value of the supernatant was measured at 540 nm on a microplate reader. The relative clotting time of each sample was determined from time *vs*. OD plots. Three parallel experiments were performed for each sample.

2.12 Fluorescent nanoprobe in cell imaging

HeLa cells were cultured as a model cell line to test the cancer targeting ability of the nanoprobe. L929 cells were cultured under the same conditions as control. Cells were cultured in DMEM supplemented with 10% fetal bovine serum (FBS), 100 μg/mL streptomycin, and 100 μg/mL penicillin at 37°C in an incubator containing 5% CO_2. The nanoprobe was sterilized by exposure to UV light for 30 min and then dispersed in DMEM. HeLa and L929 cells were cultured for 24 h to allow cell adhesion. HeLa cells were then treated by culture with 1 mL HA solution (0.05 mg/mL) in carbon dioxide incubator for 2 h. Afterwards, the nanoprobe suspension in DMEM (0.05 mg/mL) was co-cultured with pretreated HeLa cells, normal HeLa cells and L929 cells for 6 h. The cells were washed 3 times using PBS (10 mM, pH 7.4). Fluorescence images of the nanoprobes were performed using a fluorescence microscope after excitation by a green excitation source.

3. Results and Discussion

3.1 Material characterization

3.1.1 Characterization of HA-NH_2

The structure of HA and HA-NH_2 was characterized by NMR spectroscopy. As shown in Fig. 1a, the peak at 1.9 ppm corresponds to N-acetyl group of HA. New peaks belonging to the methylene group of EDA are detected at 3.0-3.2 ppm in the spectrum of aminated HA, indicating the successful modification of HA by EDA.[30] In contrast, the peaks appearing in the range of 2.7-3.0 ppm are those of ethylenediamine. Based on the peak areas at 3.0-3.2 and 1.9 ppm, the degree of functionalization in aminated HA was estimated to be 66%.

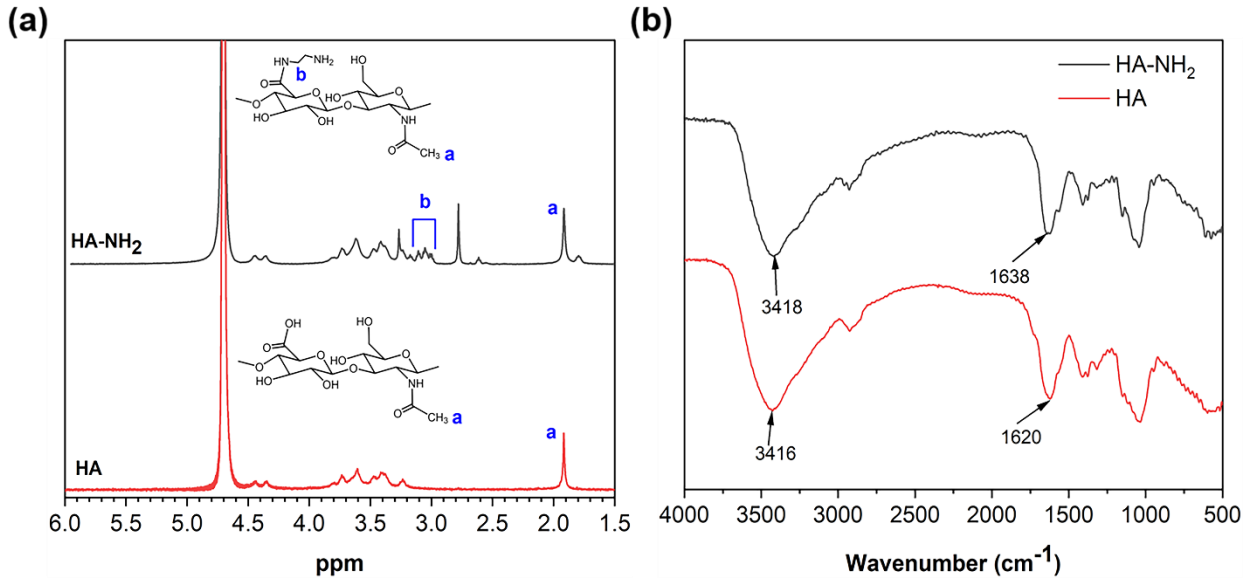

Figure 1. (a) ^{1}H-NMR spectra of HA and HA-NH_2 in D_2O, and (b) FT-IR spectra of HA and HA-NH_2.

The FTIR spectra of HA and HA-NH_2 are shown in Fig. 1b. HA is a linear polysaccharide with a large number of OH and NH groups which are observed at 3416 cm^{-1}. Another characteristic peak

detected at 1620 cm^{-1} belongs to the asymmetric carbonyl stretching vibration. The spectrum of HA-NH_2 is almost identical to that of HA. However, the characteristic absorption at 1620 cm^{-1} of HA slightly shifts to 1638 cm^{-1}, suggesting the functionalization of HA by EDA.[31]

3.1.2 Characterization of GOP and GOP-HA

It is well known that oxygen containing groups such as hydroxyl, carboxyl and epoxy are present on the surface and edge of GO,[32] while PEI and HA contain large number of amine and carboxyl groups,[33] respectively. GO-PEI (GOP) was synthesized by reaction of the carboxyl groups of GO and amine groups of PEI using EDC/NHS as coupling agents. PEI with Mw of 1800 was use because of its lower toxicity as compared to high Mw PEI.[24] HA was then attached to GOP by reaction of the carboxyl groups of HA and amine groups of PEI.

Fig. 2a presents the UV-Vis-NIR spectra of GO and GOP. GO exhibits characteristic absorption peaks at 230 and 305 nm which are attributed to the transition of C=C bonds on aromatic ring and C=O bond in carboxyl group, respectively. In contrast, the UV-Vis-NIR curve of GOP has a characteristic absorption at 260 nm, indicating that the reaction between GO and PEI leads to a red shift of absorption of C=C bonds.[34]

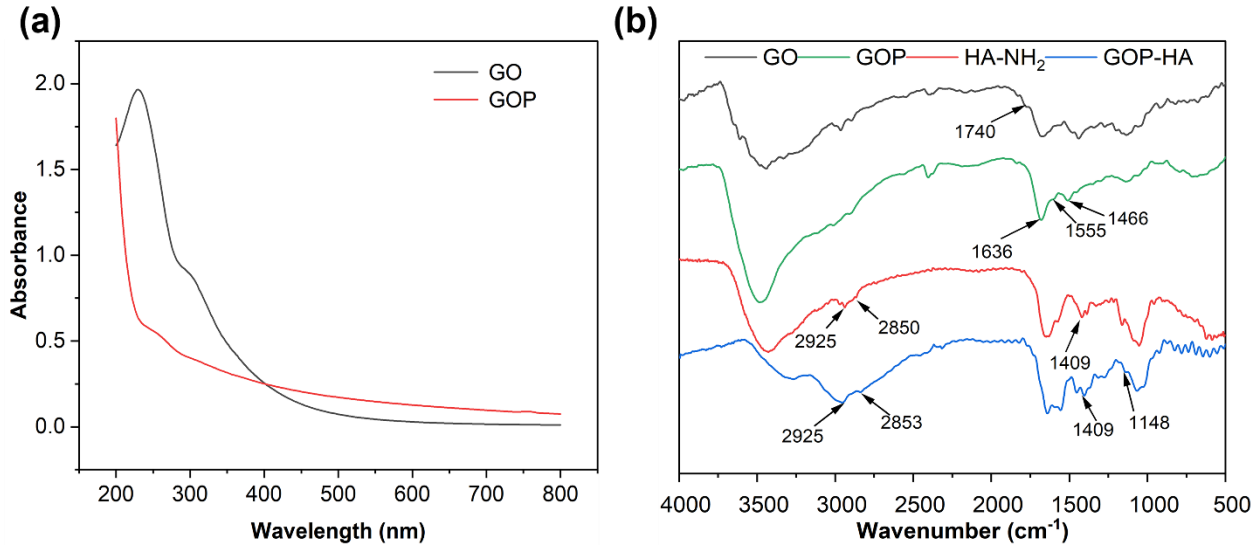

Figure 2. (a) UV-Vis-NIR spectra of GO and GOP, and (b) FT-IR spectra of GO, HA-NH_2, GOP and GOP-HA.

Fig. 2b shows the FT-IR spectra of GO, GOP, HA-NH_2 and GOP-HA. GO surface is rich in oxygen-containing functional groups, and stretching vibration bands of C-O, C-O-C, C-OH, C=O and OH are observed at 1096, 1233, 1402, 1740, and 3450 cm^{-1}, respectively.[35] The absorption peak at 1636 cm^{-1} belongs to the bending vibration of the aromatic C=C bond. The small peak at 1740 cm^{-1} disappears on the spectrum of GOP. At the same time, new absorption peaks appear at 1555 and 1466 cm^{-1}, corresponding to bending vibration of primary amine (-NH_2) and C-N stretching vibration, respectively. These findings suggest that GO has been successfully connected to PEI via amide formation. GOP-HA has characteristic absorption peaks of HA-NH_2 at 1409, 2925 and 2850 cm^{-1} belonging to C-O stretching vibration, antisymmetric absorption peaks of CH_3 and CH_2, respectively.[36] Due to the formation of the amide group, the N-H in-plane bending vibration peak of GOP at 1095 cm^{-1} exhibits a red shift to 1148 cm^{-1}, indicating a reaction between GOP and HA. Therefore, infrared spectroscopy confirmed the successful synthesis of GOP and GOP-HA.

The surface chemical composition of GO and GOP was further analyzed by XPS as shown in Fig. 3. The main difference between the spectra of GO and GOP is the presence of N 1s peak (394-398 eV) from GOP (Fig. 3a), suggesting the attachment of PEI on GO surface. In addition, the oxygen peak intensity of GOP is lower than that of GO, in agreement with the partial reduction of GO by PEI. The carbon and nitrogen elements in GO and GOP were further analyzed from high-resolution C 1s and N 1s spectra. The C 1s spectrum of GO shows the characteristic peaks of C-C, C-O, C=O and O-C=O at 282.61, 284.6, 285.02 and 286.59 eV (Fig. 3b), respectively, whereas the

C 1s spectrum of GOP shows a new peak of C-N at 282.7 eV (Fig. 3c). On the other hand, the N 1s spectrum of GOP shows a peak at 397.12 eV attributed to the amide groups, and a peak at 396.2 eV to the amine groups in PEI (Fig. 3d). Therefore, XPS results further confirmed the formation of amide bond between GO and PEI.[37-39]

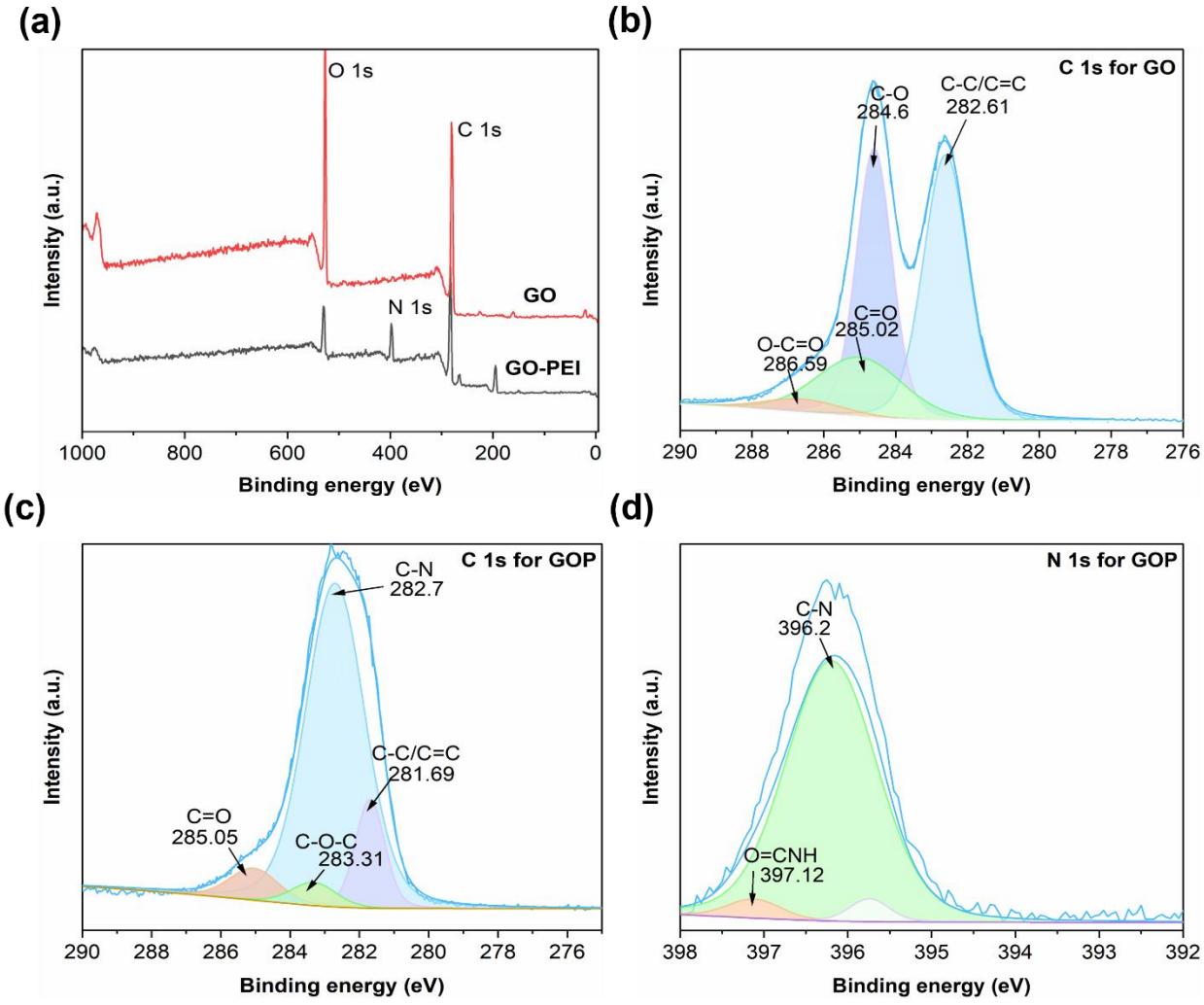

Figure 3. (a) XPS survey spectra of GO and GOP, (b) XPS spectrum of GO-C 1s, (c) XPS spectrum of GOP-C 1s, and (d) XPS spectrum of GOP-N 1s.

The morphology of GOP and GOP-HA was examined by TEM as shown in Fig. 4a and Fig. 4b. Both GOP and GOP-HA exhibit a layered structure, which is characteristic of the structure of graphene. The particle size is about 500 nm. No significant difference is observed between the surface morphologies of GOP and GOP-HA.

The zeta potential of GO, GOP and GOP-HA was measured under neutral conditions, as shown in Fig. 4c. The zeta potential of GO is -45.5 mV due to the presence of -COOH groups. In contrast, the zeta potential of GO-PEI is 19.0 mV, in agreement with the attachment of positively charged PEI [40,41]. After modification with HA-NH_2 whose zeta potential is -15 mV, the zeta potential of GOP-HA slightly decreases to 13.9 mV because the reaction between the -COOH of HA and -NH_2 of GOP decreases the number of -NH_2 functional groups at the particle surface and that the presence of HA shields part of the effect of -NH_2.

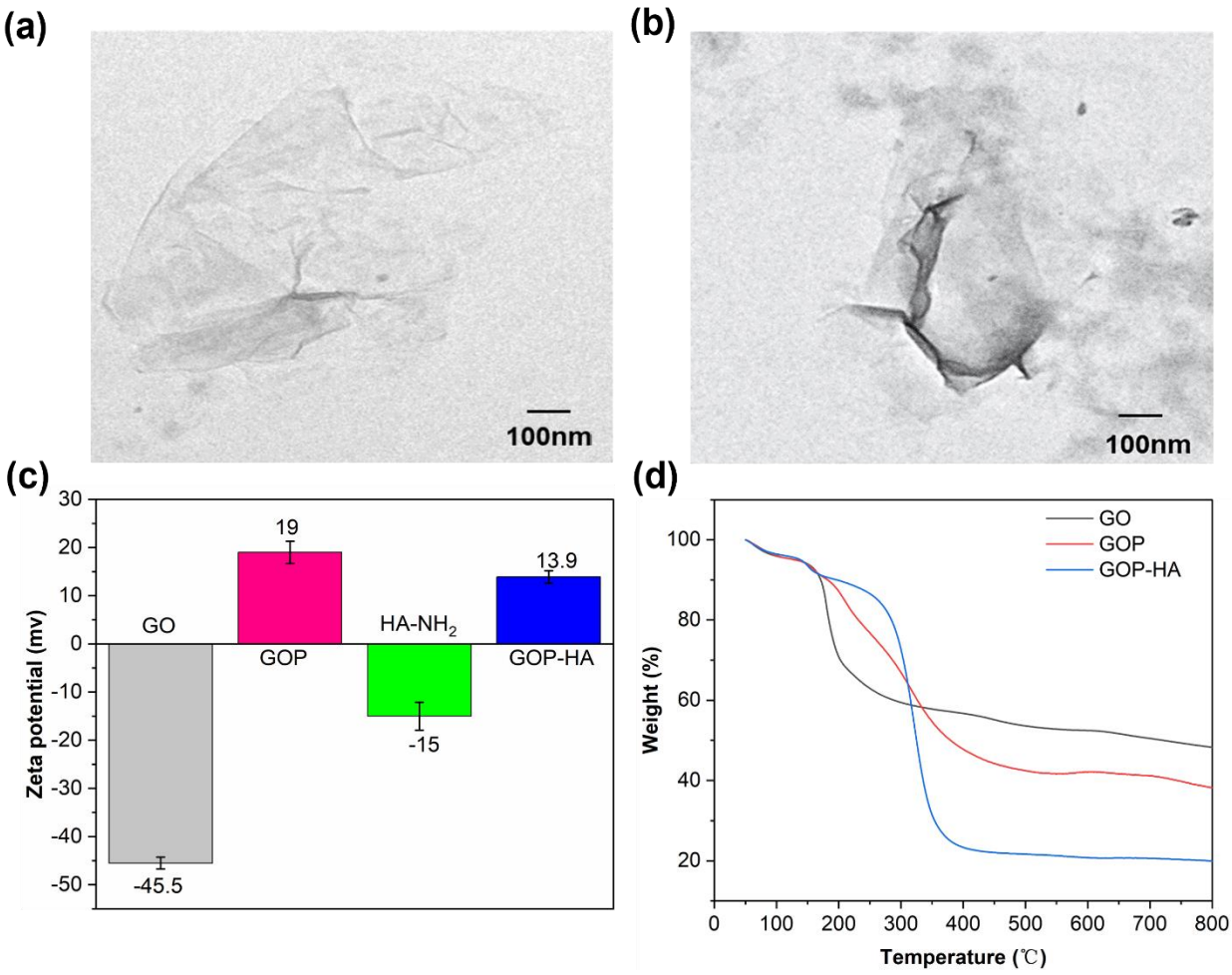

Figure 4. TEM images of (a) GOP and (b) GOP-HA; (c) Zeta potential of GO, GOP, HA-NH_2 and GOP-HA (n=3); (d) TGA thermograms of GO, GOP and GOP-HA.

Fig. 4d presents the TGA thermograms of GO, GO-PEI and GOP-HA. All three materials exhibit an initial weight loss of about 7% at 120 °C, which is attributed to the presence of water. The GO curve shows a second weight loss beyond 150°C, which reaches 45% at 450°C. This is caused by the cleavage of oxygen-containing groups. Compared with the GO curve, GOP exhibits a more progressive second weight loss phase from 150°C to 450°C, with a weight loss of about 55%. The weight loss of GOP is 10% higher than that of GO due to grafted PEI. The thermal stability of GOP-HA appears higher than that of GO and GOP as the second weight loss begins beyond 250°C,

which could be assigned to the higher thermal stability of PEI and HA as compared to GO. Weight loss of GOP-HA reaches 80% at 450°C, which is 25% higher than that of GOP due to the decomposition of PEI/HA grafted polymers.

3.2 Characterization of GOP-HA-FITC nanoprobe

FITC is widely used to label proteins by reaction of its isothiocyanate group with amino termini and primary amines in proteins [42]. In this work, amino-functionalized HA was first synthesized, HA and GOP were then linked, and finally the isothiocyanate group of FITC was used to react with the amino group in HA to generate GOP-HA-FITC nanoprobe. The nanoprobe was characterized from various aspects, including colloidal stability, effect of incubation time and enzyme concentration, fluorescence quenching, and selectivity in the presence of potential interfering substances.

3.2.1 Fluorescence quenching tests

Fluorescence quenching of the probe was confirmed from fluorescence measurements. Fig. 5a shows the fluorescence emission spectra of FITC, GOP-HA-FITC probe with hyaluronidase after 3 h incubation, GOP-HA-FITC probe, and GOP-HA-FITC after 3 h. FITC shows strong fluorescence emission at 520 nm. In contrast, GOP-HA-FITC nanoprobe showed very weak fluorescence due to fluorescence quenching. After 3 h incubation with hyaluronidase, HA is cleaved into small fragments by the enzyme, resulting in the release of FITC and the recovery of fluorescence. In contrast, the fluorescence intensity of the GOP-HA-FITC nanoprobe remains almost the same after 3 h incubation without enzyme, indicating that the fluorescence of FITC was successfully quenched in the probe.

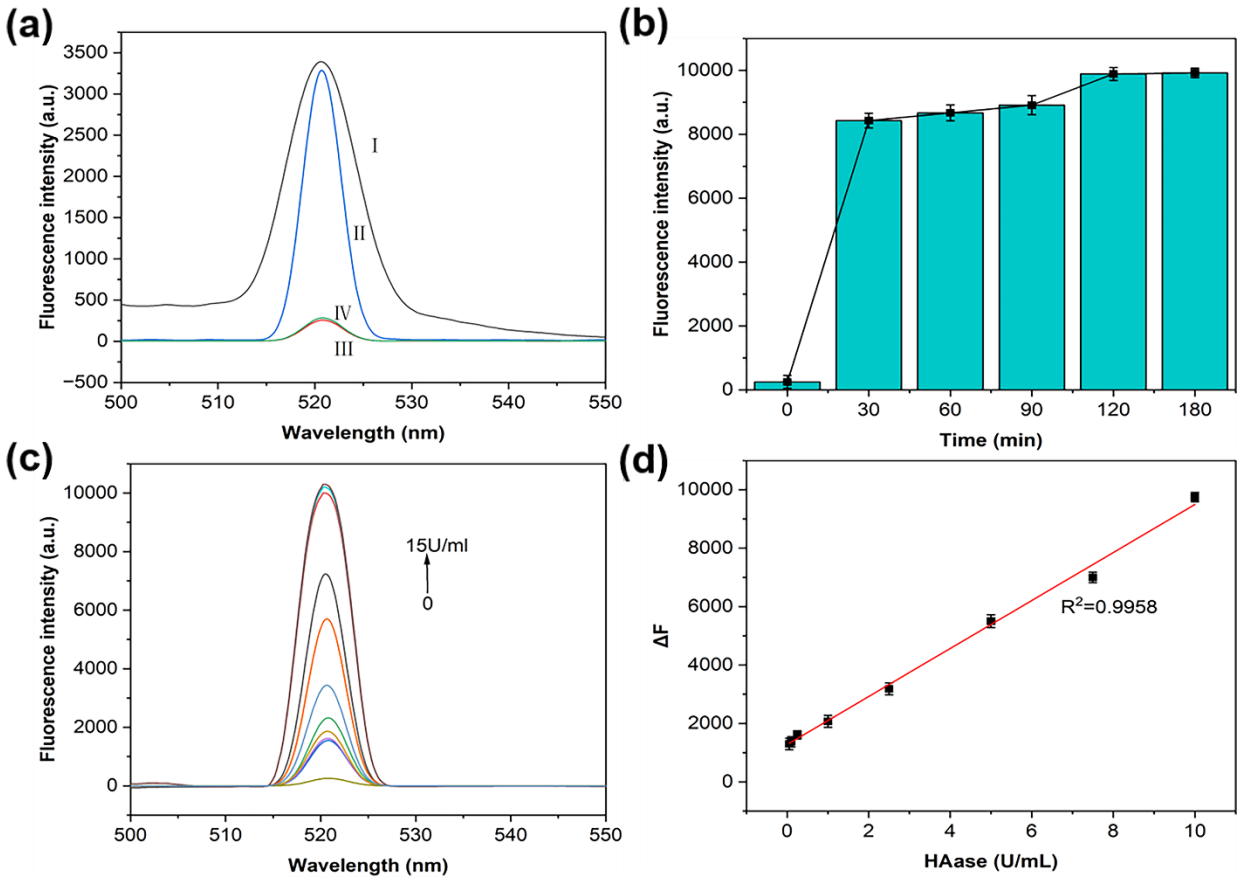

Figure 5. (a) Fluorescence emission spectra (λ ex = 490 nm): (I) FITC (0.05 mg/mL), (II) GOP-HA-FITC (0.05 mg/mL) and hyaluronidase (2.5 U/mL) after 3 h incubation, (III) GOP-HA-FITC (0.05 mg/mL), (IV) GOP-HA-FITC (0.05 mg/mL) after 3 h; (b) Fluorescence intensity detected by reaction of hyaluronidase (10 U/mL) and GOP-HA-FITC probe (0.05 mg/mL) at different times; (c) Fluorescence emission spectra (λex = 490 nm) of nanoprobe after 3 h incubation with hyaluronidase at various concentrations (0, 0.05, 0.1, 0.25, 1, 2.5, 5, 7.5, 10, 12.5 and 15 U / mL from bottom to top); (d) ΔF *vs.* HAase concentration plot in the 0.05 to 10 U/mL range (ΔF is the difference of fluorescence intensity in the presence and absence of nanoprobe). Data are expressed as the mean ± standard deviation of three measurements.

3.2.2 Effect of incubation time

The GOP-HA-FITC probe was incubated in the presence of hyaluronidase for various times up to 180 min in order to elucidate the effect of incubation time on the fluorescence intensity. As shown in Fig. 5b, the fluorescence intensity strongly increases from 260 initially to 8500 at 30 min. Thereafter, the fluorescence intensity slightly increases to 8600 at 90 min, and to 10000 at 120 min. The intensity at 180 min is almost the same as that at 120 min, indicating that a maximum of fluorescence intensity is reached beyond 120 min. An incubation time of 180 min was used for further analyses.

3.2.3 Effect of hyaluronidase concentration

GOP-HA-FITC nanoprobe (0.05 mg/mL) was incubated with hyaluronidase at different concentrations in the dark for 3 h to evaluate its sensitivity. As shown in Fig. 5c, the fluorescence intensity measured at the emission wavelength of 520 nm gradually increases with increasing enzyme concentration up to 10 U/mL, indicating that the nanoprobe has a good sensitivity in this concentration range. However, beyond 10 U/mL, the fluorescence intensity remains almost unchanged. As described above, FITC is released after hydrolysis of HA chains by hyaluronidase, resulting in fluorescence recovery. These findings indicate that the fluorescence intensity reaches a maximum at an enzyme concentration of 10 U/mL as all FITC molecules are released.

Fig. 5d shows the ΔF ($\Delta F = F - F_0$) *vs.* HAase concentration plot in the range of 0.05 to 10 U/mL. F and F_0 are the fluorescence intensities in the presence and absence of HAase, respectively. A good linearity is obtained for the plot (regression coefficient $R^2 = 0.99452$). The limit of detection (LOD) was estimated to be 0.04 U/mL, which was calculated based on the signal-to-noise ratio S/N = 3. Table 1 summarizes comparatively the performances (LOD, linear range, response time)

of GOP-HA-FITC and other fluorescent probes for hyaluronidase detection. The overall performance of GOP-HA-FITC is comparable to, or even higher than that some of reported HAase detection strategies, thus showing its potential in bioanalysis and intracellular bioimaging assay.

Table 1. Comparison of the performances between GOP-HA-FITC nanoprobe and other fluorescent probes for hyaluronidase detection

Fluorescent probe	Linear range (U/mL)	Response time (min)	Limit of detection (U/mL)	Reference
(TPE-2N, AN-N)-HA	0.005-10	100	0.0017	43
P-CD/HA-Dox	0-400	40	0.65	16
HA-UCNPs-PMPD	0-300	50	0.6	15
MoS_2QDs-(HA-AuNPS)	1-50	-	0.7	13
SiNPs-(HA-AuNPS)	0.01-10	45	0.004	14
FITC-HA-AuNPs	1.25-50	180	0.625	27
HA-ADH-FITC/HA-CHO@AuNPs	0.5-100	-	0.14	44
CQD/Naphthalimide/HA	0.1-16	80	0.09	45
Polycation1-HA/ Polycation1-QDS	0-0.1	40	0.01	46
N-Py-HA	0-3	90	0.007	47
GOP-HA-FITC	0.05-10	30	0.04	This work

3.2.4 GOP-HA-FITC stability tests

The colloidal stability of GOP-HA-FITC nanoprobe is of key importance as it is intended for intravenous applications. Stability tests were made by fluorescence intensity measurements of nanoprobe solutions (0.05 mg/mL) after 3 h incubation with hyaluronidase under different conditions, i.e. presence of salts, culture media, pH and UV light irradiation time. As shown in Fig. 6a, after 3 h incubation with hyaluronidase, the fluorescence intensity of GOP-HA-FITC probe is almost the same in the presence of NaCl at different concentrations up to 1000 mM. Similar fluorescence intensity values were also found for different complete media, i.e., PBS, DMEM, and RPMI-1640

medium (Fig. 6b). The effect of pH was considered using PBS solutions in the pH range from pH 3 to 8. The fluorescence intensity of GOP-HA-FITC probe in PBS of different pH has little difference (Fig. 6c), indicating that the effect of pH on the probe is very small in the studied pH range. Finally Fig. 6d shows that UV irradiation for different times up to 180 min has little effect on the nanoprobe. Therefore, data shown in Fig. 6 well illustrate the colloidal stability of the nanoprobe. The addition of the enzyme can produce approximately the same intensity of fluorescence under different concentrations of salt solutions, different media, different pH and different UV light irradiation times.

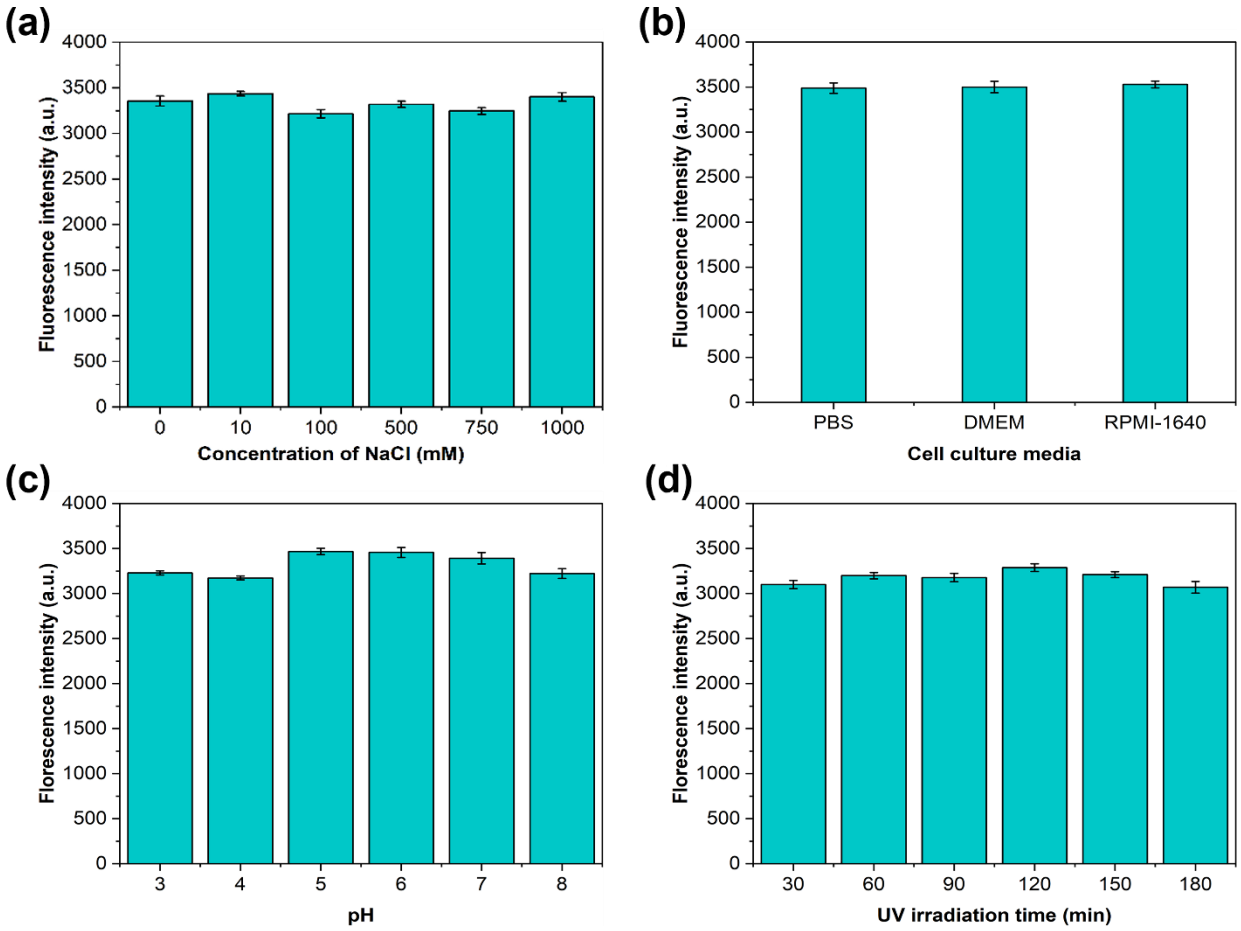

Figure 6. Fluorescence intensity of GOP-HA-FITC probe (0.05 mg/mL) after 3 h incubation with hyaluronidase (2.5 U/mL): (a) NaCl solutions at different concentrations, (b) different complete

culture media, (c) PBS solutions with different pH values, (d) UV light irradiation for different times. Data are expressed as the mean ± standard deviation of three measurements.

3.2.5 Selectivity of the nanoprobe

The nanoprobe (0.05 mg/mL) was incubated with various potential interfering substances at 37 ℃ for 3 h, including inorganic salts (NaCl, KCl, $MgCl_2$, $CaCl_2$), cysteine, glucose, vitamin B1, BSA and some enzymes (trypsin, collagenase, lysozyme, protease K) in order to demonstrate the selectivity of nanoprobe for hyaluronidase. As shown in Table 2, the fluorescence intensity of the nanoprobe is 3118.1 after incubation with hyaluronidase, which is much higher than the values obtained for potential interfering substances. These findings suggest that the nanoprobe has a good selectivity for hyaluronidase which is capable of cleaving the HA chain of the substrate.

Table 2. Comparison of the fluorescence intensity GOP-HA-FITC probe after incubation with hyaluronidase and potential interfering substances

Interfering substances	Amount added	Fluorescence intensity *
None	0	152.2 ± 7.1
NaCl	10 mM	99.1 ± 5.7
KCl	10 mM	93.2 ± 6.6
$MgCl_2$	10 mM	167.6 ± 16.3
$CaCl_2$	10 mM	122.8 ± 15.0
Cysteine	30 μM	107.3 ± 11.6
Glucose	30 μM	110.2 ± 11.7
Vitamin B1	10 mM	130.8 ± 2.9
BSA	10 mM	203.6 ± 3.8
Trypsin	2.5 U/mL	188.8 ± 78.2
Collagenase	2.5 U/mL	173.2 ± 6.8
Lysozyme	2.5 U/mL	149.6 ± 12.9
Protease K	2.5 U/mL	168.6 ± 25.6
HAase	2.5 U/mL	3118.1 ± 11.8

462 * Data are expressed as the mean ± standard deviation of three measurements.

463

464 **3.3 Cytocompatibility and haemocompatibility**

465 MTT assay was used to assess the cytotoxicity of GOP-HA-FITC nanoprobe using L929 cell
466 line. The cell viability was evaluated from the ratio of cells incubated with GOP-HA-FITC nano-
467 probe to those with the negative control. As shown in Fig. 7a-b, GOP-HA-FITC nanoprobe exhibits
468 little cytotoxicity. In the concentration range of 10 to 100 μg/mL up to 72 h incubation, the cell
469 viability is higher than 83%. These findings show that the nanoprobe presents good cytocompati-
470 bility, and thus has great potential in biological imaging applications under physiological condi-
471 tions.

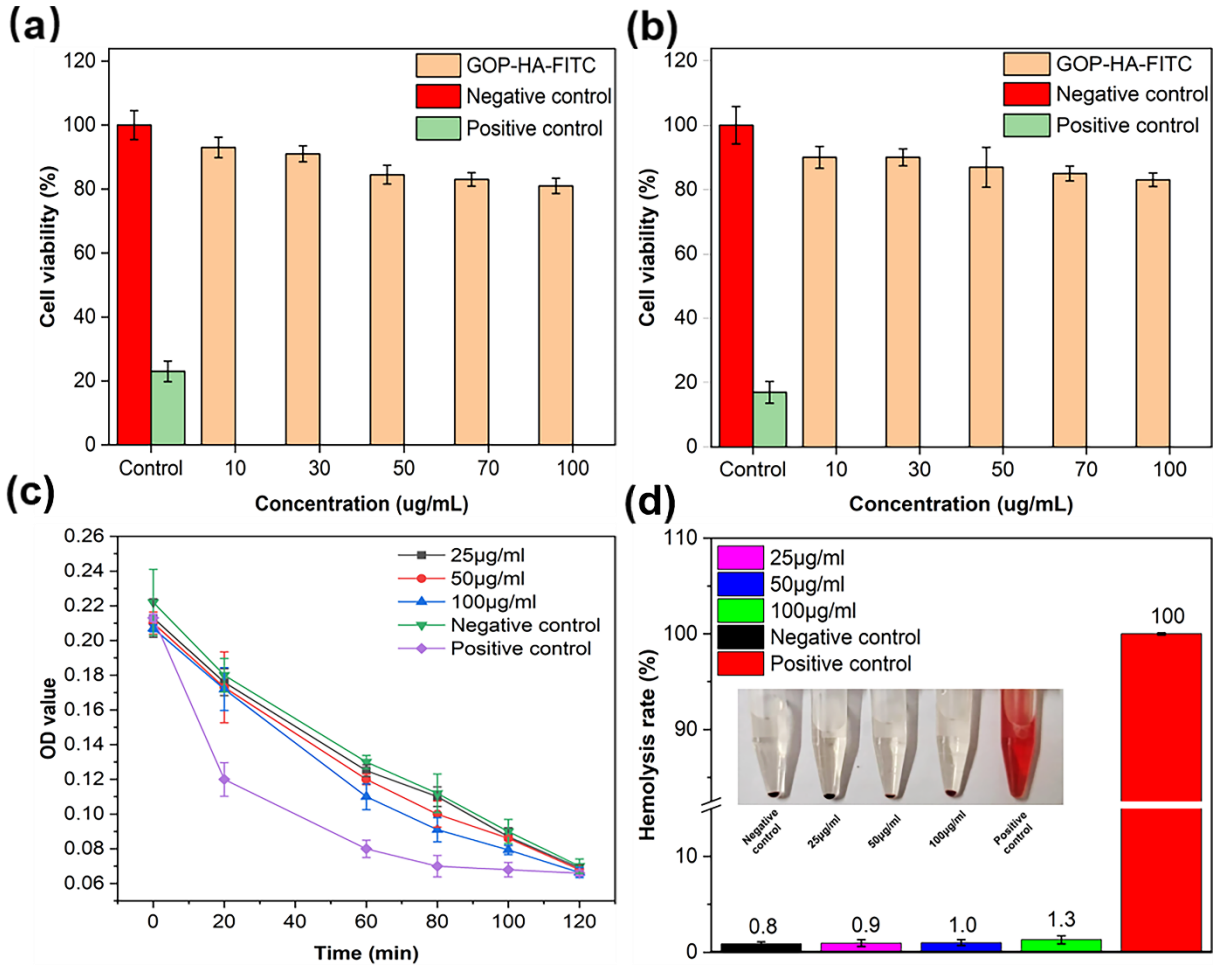

472

Figure 7. Cell viability of L929 cells after co-culture with GOP-HA-FITC probes at different concentrations after (a) 24 h, and (b) 72 h; (c) absorbance changes of the probe at different concentrations in comparison with the controls; (d) hemolysis rates (HR) of the probe at different concentrations in comparison with the controls. Data are expressed as the mean ± standard deviation of three measurements.

The haemo-compatibility of the GOP-HA-FITC probe was of key importance as the probe is intended to be applied by intravenous injection. Dynamic coagulation and hemolysis experiments were performed using rabbit blood. Fig. 7c shows the blood absorbance changes of the probe at different concentrations in comparison with the controls. The absorbance of the positive control decreases rapidly within the first 20 min, followed by slower decrease up to 120 min. The absorbance values at 60 to 120 min are almost the same, i.e. the total blood clotting time is 60 min. The absorbance changes of the probe are similar to those of the negative result. The absorbance decreases slowly, and reaches coagulation at 120 min. The above results show that the probe does not cause blood coagulation, indicating that it could be used as a biomaterial. [48]

Fig. 7d shows the hemolysis rates (HR) of the probe at different concentrations in comparison with the negative control. The HR values are in the range of 0.9 to 1.3. It is commonly admitted that the hemolytic property of biomaterials is acceptable for medical applications if the HR value is below 5%. Therefore, the HR values of the probe are all well below 5%, in agreement with the excellent anti-hemolysis properties.

3.4 Cell imaging

CD44 is a type I transmembrane glycoprotein overexpressed on the cytoplasmic membrane of a variety of tumors. [49] HA is known for its high affinity to tumor cells overexpressing CD44 receptor. [50] HeLa cells were used as a model cell line to examine the cancer targeting ability of GOP-HA-FITC nanoprobe. HeLa cells were first treated with a HA solution. Reaction of HA with CD44 receptor on the surface of HeLa cells allowed subsequent comparison with HeLa cells that were not pretreated with HA.

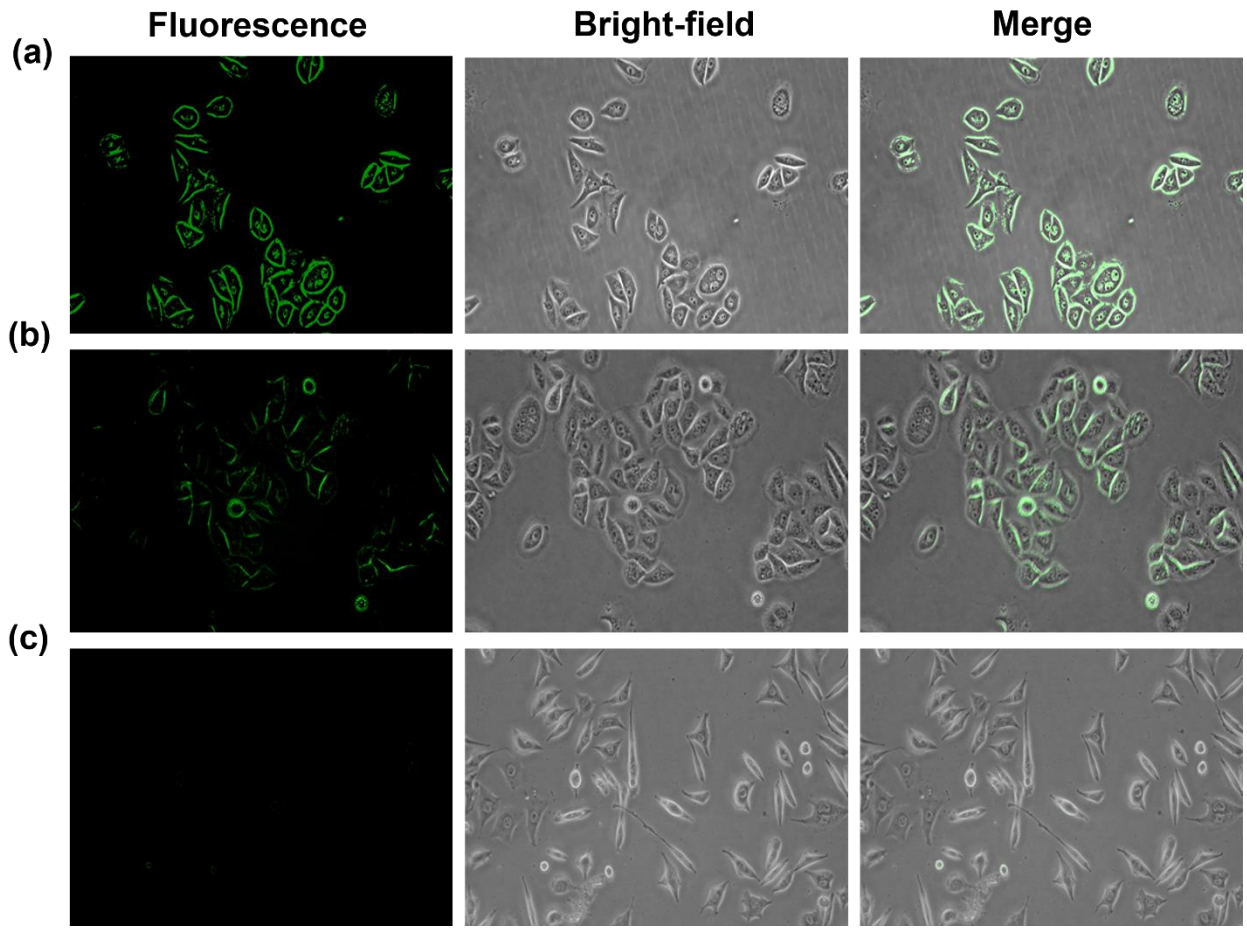

Figure 8. (a) Fluorescence images of HeLa cells after incubation with GOP-HA-FITC probe, (b) fluorescence images of HeLa cells pretreated with HA after incubation with GOP-HA-FITC nano-probe, (c) fluorescence images of L929 cells after incubation with GOP-HA-FITC probe. The first column represents the fluorescence image of cells, the second column represents the image of cells under the bright field of view, and the third column represents the combined image of both.

As shown in Fig. 8, the nanoprobe can target cancer cells thanks to the specific affinity of HA for CD44 receptor. After incubation with GOP-HA-FITC nanoprobe, HeLa cells clearly showed significant green fluorescence under fluorescence microscope due to the fluorescence emitted by FITC (Fig. 8a). Green fluorescence is clearly visible in the cell membrane and nucleus, indicating that the nanoprobe was internalized into HeLa cells and FITC was released after HA chain cleavage by hyaluronidase. In fact, two homologous hyaluronidase isoforms, namely hyaluronidase-1 (Hyal-1) and hyaluronidase-2 (Hyal-2), are predominately involved in the cellular HA catabolism in the human body.[51] Hyal-2 is mainly located on the external surface of the cell membrane, whereas Hyal-1 is identified as the major tumor-derived hyaluronidase expressed in some cancer tissues. Thus this finding should not affect the sensitivity and selectivity of the nanoprobe as both Hyal-1 and Hyal-2 can be detected. On the other hand, the fluorescence of HeLa cells pretreated with HA is weaker (Fig. 8b), suggesting that pretreatment of Hela cells with HA reduced the nanoprobe's targeting efficiency because of less CD44 receptors and hyaluronidase remaining on the cell surface. In L929 cells, there is only very weak fluorescence on the outer membrane, but there is no fluorescence inside (Fig. 8c), indicating that the nanoprobe has no effect on normal cells. These results suggest that GOP-HA-FITC nanoprobe can selectively bind to CD44 receptor and be internalized into cancer cells through receptor targeted endocytosis. Therefore, GOP-HA-FITC nanoprobe could present great potential for uses in targeted tumor cell imaging.

4. Conclusion

A novel fluorescence-quenched GOP-HA-FITC nanoprobe was successfully synthesized by successive attachment of PEI, HA and FITC to GO nanoparticles via covalent linkage. The nanoprobe exhibits high sensitivity and selectivity, and can enter cancer cells through the specific binding of

HA to cancer cells. After hydrolytic cleavage of HA chains by the overexpressed hyaluronidase, FITC is released from the probe and its fluorescence recovered, showing strong fluorescence intensity in cancer cells. Moreover, the probe presents outstanding cyto- and haemo-compatibility. Therefore, it is concluded that the developed GOP-HA-FITC nanoprobe can be used for tumor-targeted cell imaging, and is thus promising for use in early tumor diagnosis.

Author information

Corresponding Authors

Feng Su - School of Chemical Engineering, Qingdao University of Science and Technology, Qingdao 266042, China; Email: sufeng@qust.edu.cn

Qian Li - Cancer Institute, Affiliated Hospital of Qingdao University, Qingdao 266071, China; Email: liqian123@qdu.edu.cn

Suming Li - Institut Européen des Membranes, IEM UMR 5635, Univ Montpellier, CNRS, ENSCM, Montpellier, France; orcid.org 0000-0002-3345-1479 ; Email: suming.li@umontpellier.fr

Present Addresses

State Key Laboratory Base of Eco-chemical Engineering, College of Chemical Engineering, Qingdao University of Science and Technology, Qingdao 266042, China

Author Contributions

Conceptualization, F. Su, Q. Li and S. Li; methodology, Q. Li, F. Su; validation, C. Zhang and J. Song; formal analysis, S. Wang; investigation, P. Zhang; curation, P. Zhang; writing—original draft preparation, P. Zhang; writing—review and editing, S. Li; funding acquisition, F. Su, S. Li. All authors have read and agreed to the published version of the manuscript.

Notes

The authors declare no competing financial interest.

Data Availability Statements

The data of our findings are available from the corresponding author upon reasonable request.

Acknowledgements

The work was financially supported by the Shandong Provincial Natural Science Foundation (ZR2020MH324, ZR2021ME208, ZR2022ME083).

ORCID

Su Ming Li orcid.org 0000-0002-3345-1479

Qian Li orcid.org 0000-0002-8573-8690

References

1. Jemal, A.; Center, M. M.; DeSantis, C.; Ward, E. M. Global patterns of cancer incidence and mortality rates and trends. CANCER EPIDEM BIOMAR 2010; 19, 1893-1907.
2. Bukowczan, J.; Pattman, S.; Jenkinson, F.; Quinton, R. Regan isoenzyme of alkaline phosphatase as a tumour marker for renal cell carcinoma. ANN CLIN BIOCHEM 2014; 51, 611-614.
3. Chai, Y.; Gao, Y.; Xiong, H.; Lv, W.; Yang, G.; Lu, C.; Nie, J.; Ma, C.; Chen, Z.; Ren, J. A near-infrared fluorescent probe for monitoring leucine aminopeptidase in living cells. Analyst 2019; 144, 463-467.
4. Walker, C.; Mojares, E.; del Río Hernández, A. Role of extracellular matrix in development and cancer progression. INT J MOL SCI 2018; 19, 3028.
5. Buhren, B.; Schrumpf, H.; Hoff, N.; Bölke, E.; Hilton, S.; Gerber, P. Hialuronidasa: desde aplicaciones clínicas hasta mecanismos moleculares y celulares. Eur J Med Res 2016; 21.
6. Beech, D. J.; Madan, A. K.; Nan, D. Expression of PH-20 in Normal and Neoplastic Breast Tissue. J SURG RES 2002; 103, 203-207.
7. Bouga, H.; Tsouros, I.; Bounias, D.; Kyriakopoulou, D.; Stavropoulos, M. S.; Papageorgakopoulou, N.; Theocharis, D. A.; Vynios, D. H. Involvement of hyaluronidases in colorectal cancer. BMC cancer 2010; 10, 1-8.
8. Godin, D. A.; Fitzpatrick, P. C.; Scandurro, A. B.; Belafsky, P. C.; Woodworth, B. A.; Amedee, R. G.; Beech, D. J.; Beckman, B. S. PH-20: a novel tumor marker for laryngeal cancer. Arch Otolaryngol Head Neck Surg 2000; 126, 402-404.
9. Vercruysse, K. P.; Lauwers, A. R.; Demeester, J. M. Absolute and empirical determination of the enzymatic activity and kinetic investigation of the action of hyaluronidase on hyaluronan using viscosimetry. BIOCHEM J 1995; 306 (Pt 1), 153.
10. Dorfman, A.; Ott, M. L. A TURBIDIMETRIC METHOD FOR THE ASSAY OF HYALURONIDASE. J BIOL CHEM 1948; 172.
11. Williams, J. M.; Stokes, J. M.; MacDonald, M. H.; Benton, H. P. Evaluation of hyaluronidase activity in equine and bovine sera and equine synovial fluid samples by use of enzyme zymography. AM J VET RES 2005; 66, 984-990.
12. Greif, R. L. Colorimetric determination of hyaluronidase activity. J BIOL CHEM 1952; 194, 619.
13. Gu, W.; Yan, Y.; Zhang, C.; Ding, C.; Xian, Y. One-step synthesis of water-soluble MoS2 quantum dots via a hydrothermal method as a fluorescent probe for hyaluronidase detection. ACS APPL MATER INTER 2016; 8, 11272-11279.
14. Ge, J.; Cai, R.; Yang, L.; Zhang, L.; Jiang, Y.; Yang, Y.; Cui, C.; Wan, S.; Chu, X.; Tan, W. Core–shell HA-AuNPs@ SiNPs nanoprobe for sensitive fluorescence hyaluronidase detection and cell imaging. ACS SUSTAIN CHEM ENG 2018; 6, 16555-16562.
15. Wang, Z.; Li, X.; Song, Y.; Li, L.; Shi, W.; Ma, H. An upconversion luminescence nanoprobe for the ultrasensitive detection of hyaluronidase. ANAL CHEM 2015; 87, 5816-5823.
16. Gao, N.; Yang, W.; Nie, H.; Gong, Y.; Jing, J.; Gao, L.; Zhang, X. Turn-on theranostic fluorescent nanoprobe by electrostatic self-assembly of carbon dots with doxorubicin for targeted cancer cell imaging, in vivo hyaluronidase analysis, and targeted drug delivery. BIOSENS BIOELECTRON 2017; 96, 300-307.

17. Yildiz, T.; Gu, R.; Zauscher, S.; Betancourt, T. Doxorubicin-loaded protease-activated near-infrared fluorescent polymeric nanoparticles for imaging and therapy of cancer. International journal of nanomedicine 2018; 13, 6961.
18. Hernandez, D. S.; Schunk, H. C.; Shankar, K. M.; Rosales, A. M.; Suggs, L. J. Poly-d-lysine coated nanoparticles to identify pro-inflammatory macrophages. Nanoscale Advances 2020; 2, 3849-3857.
19. Daniyal, M.; Liu, B.; Wang, W. Comprehensive review on graphene oxide for use in drug delivery system. CURR MED CHEM 2020; 27, 3665-3685.
20. Ge, K.; Zhang, Y.; Wang, D.; Li, Z.; Zhu, L. Highly Stable Reduced Graphene Oxide Wrapped Black Phosphorus Heterostructure with Superior Photocatalytic Performance under Visible Light. ACS APPL MATER INTER 2020; 12.
21. Verde, V.; Longo, A.; Cucci, L. M.; Sanfilippo, V.; Magrì, A.; Satriano, C.; Anfuso, C. D.; Lupo, G.; La Mendola, D. Anti-angiogenic and anti-proliferative graphene oxide nanosheets for tumor cell therapy. INT J MOL SCI 2020; 21, 5571.
22. Zhang, Q.; Huang, X.; Pu, Y.; Yi, Y.; Zhang, T.; Wang, B. pH-sensitive and biocompatible quercetin-loaded GO–PEA–HA carrier improved antitumour efficiency and specificity. ARTIF CELL NANOMED B 2018; 46, S28-S37.
23. Bahulekar, R.; Ayyangar, N.; Ponrathnam, S. Polyethyleneimine in immobilization of biocatalysts. ENZYME MICROB TECH 1991; 13, 858-868.
24. Godbey, W.; Wu, K. K.; Mikos, A. G. Size matters: molecular weight affects the efficiency of poly (ethylenimine) as a gene delivery vehicle. Journal of Biomedical Materials Research: An Official Journal of The Society for Biomaterials, The Japanese Society for Biomaterials,The Australian Society for Biomaterials 1999; 45, 268-275.
25. F Rodrigues, C.; Fernandes, N.; de Melo-Diogo, D.; Ferreira, P.; J Correia, I.; F Moreira, A. HA/PEI-coated acridine orange-loaded gold-core silica shell nanorods for cancer-targeted photothermal and chemotherapy. Nanomedicine 2021; 16, 2569-2586.
26. Hsu, S.-h.; Yu, A.; Yeh, C.-A.; Sun, W.-S.; Lin, S.-Z.; Fu, R.-H.; Hsieh, H.-H.; Wu, P.-Y.; Hung, H.-S. Biocompatible nanogold carrier coated with hyaluronic acid for efficient delivery of plasmid or siRNA to mesenchymal stem cells. ACS Appl Bio Mater 2019; 2, 1017-1030.
27. Cheng, D.; Han, W.; Yang, K.; Song, Y.; Jiang, M.; Song, E. One-step facile synthesis of hyaluronic acid functionalized fluorescent gold nanoprobes sensitive to hyaluronidase in urine specimen from bladder cancer patients. Talanta 2014; 130, 408-414.
28. Moreton, S.; Faulds, K.; Shand, N. C.; Bedics, M. A.; Detty, M. R.; Graham, D. Functionalisation of hollow gold nanospheres for use as stable, red-shifted SERS nanotags. NANOSCALE 2015; 7, 6075-6082.
29. Thierry, B.; Kujawa, P.; Tkaczyk, C.; Winnik, F. M.; Bilodeau, L.; Tabrizian, M. Delivery platform for hydrophobic drugs: prodrug approach combined with self-assembled multilayers. J AM CHEM SOC 2005; 127, 1626-1627.
30. Hu, D.; Zhong, L.; Wang, M.; Li, H.; Qu, Y.; Liu, Q.; Han, R.; Yuan, L.; Shi, K.; Peng, J. J. A. F. M. Perfluorocarbon‐loaded and redox‐activatable photosensitizing agent with oxygen supply for enhancement of fluorescence/photoacoustic imaging guided tumor photodynamic therapy. 2019; 29, 1806199.
31. Ling, X.; Zhao, C.; Huang, L.; Wang, Q.; Tu, J.; Shen, Y.; Sun, C. Synthesis and characterization of hyaluronic acid–platinum (iv) nanoconjugate with enhanced antitumor

response and reduced adverse effects. RSC ADV 2015; 5, 81668-81681.
32. Bonanni, A.; Chua, C. K.; Pumera, M. Rational design of carboxyl groups perpendicularly attached to a graphene sheet: a platform for enhanced biosensing applications. Chemistry–A European Journal 2014; 20, 217-222.
33. Sionkowska, A.; Gadomska, M.; Musiał, K.; Piątek, J. Hyaluronic acid as a component of natural polymer blends for biomedical applications: a review. MOLECULES 2020; 25, 4035.
34. Ou, L.; Lin, H.; Song, Y.; Tan, G.; Gui, X.; Li, J.; Chen, X.; Deng, Z.; Lin, S. Efficient miRNA Inhibitor with GO-PEI Nanosheets for Osteosarcoma Suppression by Targeting PTEN. INT J NANOMED 2020; 15, 5131.
35. Marcano, D. C.; Kosynkin, D. V.; Berlin, J. M.; Sinitskii, A.; Sun, Z.; Slesarev, A.; Alemany, L. B.; Lu, W.; Tour, J. M. Improved synthesis of graphene oxide. ACS NANO 2010; 4, 4806-4814.
36. Alkrad, J. A.; Mrestani, Y.; Stroehl, D.; Wartewig, S.; Neubert, R. Characterization of enzymatically digested hyaluronic acid using NMR, Raman, IR, and UV–Vis spectroscopies. JPBA 2003; 31, 545-550.
37. Su, X.; Liang, J.; Yang, L.; Hu, Q.; Shan, X.; Wan, J.; Hu], Z. Synthesis of polymer-functionalized nanoscale graphene oxide with different surface charge and its cellular uptake, biosafety and immune responses in Raw264.7 macrophages. MAT SCI ENG C 2018.
38. Li, T.; Wu, L.; Zhang, J.; Xi, G.; Pang, Y.; Wang, X.; Chen, T. Hydrothermal Reduction of Polyethylenimine and Polyethylene Glycol Dual-Functionalized Nanographene Oxide for High-Efficiency Gene Delivery. ACS APPL MATER INTER 2016, acsami.6b09915.
39. Zhang, L.; Chen, B.; Ghaffar, A.; Zhu, X. Nanocomposite Membrane with Polyethylenimine-grafted Graphene Oxide as a Novel Additive to Enhance Pollutant Filtration Performance. ENVIRON SCI TECHNOL 2018; 52, 5920-5930.
40. Dong, C.; Wang, Y.; Gonzalez, G. X.; Ma, Y.; Song, Y.; Wang, S.; Kang, S.-M.; Compans, R. W.; Wang, B.-Z. Intranasal vaccination with influenza HA/GO-PEI nanoparticles provides immune protection against homo-and heterologous strains. PNAS 2021; 118.
41. Xu, L.; Xiang, J.; Liu, Y.; Xu, J.; Luo, Y.; Feng, L.; Liu, Z.; Peng, R. Functionalized graphene oxide serves as a novel vaccine nano-adjuvant for robust stimulation of cellular immunity. NANOSCALE 2016; 8, 3785-3795.
42. Jang, J. H.; Lim, H. B. Characterization and analytical application of surface modified magnetic nanoparticles. Microchem J 2010; 94, 148-158.
43. Xie, H.; Zeng, F.; Wu, S. Ratiometric fluorescent biosensor for hyaluronidase with hyaluronan as both nanoparticle scaffold and substrate for enzymatic reaction. Biomacromolecules 2014; 15, 3383-3389.
44. Ge, M.; Sun, J.; Chen, M.; Tian, J.; Yin, H.; Yin, J. J. A.; chemistry, b. A hyaluronic acid fluorescent hydrogel based on fluorescence resonance energy transfer for sensitive detection of hyaluronidase. Analytical bioanalytical chemistry 2020; 412, 1915-1923.
45. Raj, P.; Lee, S.-y.; Lee, T. Y. Carbon dot/naphthalimide based ratiometric fluorescence biosensor for hyaluronidase detection. Materials 2021; 14, 1313.
46. Wang, Y.; Gao, W. A label-free and sensitive fluorescence assay for hyaluronidase activity through electrostatic-controlled quantum dots self-assembly. Journal of Chemical Research 2021; 45, 896-902.
47. Hu, Q.; Zeng, F.; Wu, S. A ratiometric fluorescent probe for hyaluronidase detection via

hyaluronan-induced formation of red-light emitting excimers. Biosensors Bioelectronics 2016; 79, 776-783.
48. Wang, C.; Zheng, Y.; Sun, Y.; Fan, J.; Qin, Q.; Zhao, Z. A novel biodegradable polyurethane based on poly (3-hydroxybutyrate-co-3-hydroxyvalerate) and poly (ethylene glycol) as promising biomaterials with the improvement of mechanical properties and hemocompatibility. Polymer Chemistry 2016; 7, 6120-6132.
49. Hassn Mesrati, M.; Syafruddin, S. E.; Mohtar, M. A.; Syahir, A. CD44: A Multifunctional Mediator of Cancer Progression. BIOMOLECULES 2021; 11, 1850.
50. Mattheolabakis, G.; Milane, L.; Singh, A.; Amiji, M. M. Hyaluronic acid targeting of CD44 for cancer therapy: from receptor biology to nanomedicine. J DRUG TARGET 2015; 23, 605-618.
51. Li, Y.; Yang, S.; Guo, L.; Xiao, Y.; Luo, J.; Li, Y.; Wong, M. S.; Yang, R. Differentiation of intracellular hyaluronidase isoform by degradable nanoassembly coupled with RNA-binding fluorescence amplification. Analytical Chemistry 2019; 91, 6887-6893.